HybridSLAM; A Robust Algorithm for Similtaneous Localization and Mapping

Amir Monjazeb[1], Jurek Z. Sasiadek[1] and Dan Necsulescu[2]
[1]*Department of Mechanical and Aerospace Engineering, Carleton University, 1125 Colonel By Drive, Ottawa, Canada*
[2]*Department of Mechanical Engineering, Ottawa University, 161 Louis Pasteur, CBY A205, Ottawa, Canada*
amonjaze@connect.carleton.ca, jsas@connect.carleton.ca, necsu@uottawa.ca

Keywords: Simultaneous Localization and Mapping (SLAM) problem, Unscented HybridSLAM, Unscented Kalman Filter, Position Error, Time and Measurement Update.

Abstract: This paper addresses an ongoing research on a novel approach to Simultaneous Localization and Mapping problem called Unscented HybridSLAM. The main contribution of this paper is to develop the map update formulas along with proof results in order to investigate the validation of the map evolution. The investigation is presented using the help of simulations in terms of robustness, map fusion, and the update process. Results clearly show that as the vehicle travels along the path and the map evolves, the Unscented HybridSLAM algorithm avoids the overestimation of landmarks.

1 INTRODUCTION

Simultaneous localization and mapping (SLAM) is well known navigation technique for quite some time (Smith, Cheesman, 1986). It is more than 2 decades that different aspects of SLAM are identified and examined using many different algorithms (Durrant-Whyte, Bailey, 2006). Such algorithms are used to solve SLAM problem in terms of ambiguity in data association and complexity in computation (Monjazeb et al., 2012). After all, the challenge is to avoid under/overestimation of path and objects in the environment. Amongst all solutions to SLAM problem, different versions of FastSLAM (Montemerlo, Thrun, 2003) and a few extensions of Kalman filter are the pioneers (Bailey, 2002). For instance, EKF-SLAM is accepted as the gold standard solution, nevertheless, under some limitations and specific circumstances. In order to overcome such limitations, there are some combined algorithms such as HybridSLAM (Brooks, 2009) that by the use map fusion techniques (Williams, et al, 2002) may be able to produce more reliable maps. In some situations, such combined filters may be superior to their counterparts. For instance, in a large environment with huge amount of landmarks, HybridSLAM outperforms FastSLAM based algorithms. In this study a combined filter called Unscented HybridSLAM and (as a combination of HybridSLAM and Unscented Kalman Filter) is represented. Then, map updating process is theoretically probed and formulated. After all, simulation of different scenarios will be presented and the mapping update steps, robustness, and different stages of map fusion process will be thoroughly investigated and discussed. The estimation of the mean and covariance of the proposed algorithm will be analyzed and the results will be compared with currently used algorithms.

2 UNSCENTED HYBRIDSLAM ALGORITHM

Same as HybridSLAM (HS), the proposed algorithm is a combination of FastSLAM and an extension of Kalman filter. In Unscented HybridSLAM (Monjazeb et al., 2014) however, the unscented Kalman filter plays a role of estimating the global map and getting updated once a local map is estimated by FastSLAM. Naturally, UHS inherits all properties of its subordinate filter UKF. As a matter of fact, UHS does not suffer from the inconsistency of EKF-SLAM the way HS does. Furthermore, UHS

is able to more properly handle the non-linearity of the system than HS. By the help of a map-fusion technique, UHS would be able to outperform EKF-SLAM, FastSLAM, and HybridSLAM. This superiority in performance specifically lies in the heart of the algorithm where time and measurement processes are carefully updated without any ambiguity. Moreover, UHS stays robust to cluttered environments (Monjazeb et al., 2011).

3 TIME AND MEASUREMENT UPDATE PROCESS

The first step is to initialize the position of the robot at time zero, the covariance matrix of the system, and noise in motion and observation as well as their covariance matrices.

$$\hat{\mathbf{x}}_0 = \mathrm{E}[\mathbf{x}_0] \qquad \mathbf{P}_{\mathbf{x}_k} = \mathbf{E}[(\mathbf{x}_0 - \hat{\mathbf{x}}_0)(\mathbf{x}_0 - \hat{\mathbf{x}}_0)^T] \tag{1}$$

$$\overline{\mathbf{w}}_k = \mathrm{E}[\mathbf{w}_k] \qquad \mathbf{Q}_{k_k} = \mathrm{E}[(\mathbf{w}_k - \overline{\mathbf{w}}_k)(\mathbf{w}_k - \overline{\mathbf{w}}_k)^T] \tag{2}$$

$$\overline{\mathbf{v}}_k = \mathrm{E}[\mathbf{v}_k] \qquad \mathbf{R}_{k_k} = \mathrm{E}[(\mathbf{v}_k - \overline{\mathbf{v}}_k)(\mathbf{v}_k - \overline{\mathbf{v}}_k)^T] \quad \text{for } k = 1 \ldots \infty \tag{3}$$

The covariance square-root column vectors for time –update [10] are

$$\mathbf{s}_{k-1}^{x,i} = \ell\left(\sqrt{\mathbf{P}_{\mathrm{x}_{k-1}}}\right)_i \qquad i = 1, 2, \ldots, L_{\mathrm{x}} \tag{4}$$

$$\mathbf{s}_{k-1}^{w,i} = \ell\left(\sqrt{\mathbf{Q}_k}\right)_i \qquad i = 1, 2, \ldots, L_{\mathrm{w}} \tag{5}$$

The time-update equations are

$$\begin{aligned}\hat{\mathbf{x}}_k^- &= \frac{\ell^2 - L_x - L_w}{\ell^2} f(\hat{\mathbf{x}}_{k-1}, \overline{\mathbf{w}}_k, \mathbf{u}_{k-1}) \\ &+ \frac{1}{2\ell^2}\sum_{i=1}^{L_x}[f(\hat{\mathbf{x}}_{k-1} + \mathbf{s}_{k-1}^{x,i}, \overline{\mathbf{w}}_k, \mathbf{u}_{k-1}) + f(\hat{\mathbf{x}}_{k-1} - \mathbf{s}_{k-1}^{x,i}, \overline{\mathbf{w}}_k, \mathbf{u}_{k-1})] \\ &+ \frac{1}{2\ell^2}\sum_{i=1}^{L_w}[f(\hat{\mathbf{x}}_{k-1}, \overline{\mathbf{w}}_k + \mathbf{s}_{k-1}^{w,i}, \mathbf{u}_{k-1}) + f(\hat{\mathbf{x}}_{k-1}, \overline{\mathbf{w}}_k - \mathbf{s}_{k-1}^{w,i}, \mathbf{u}_{k-1})]\end{aligned} \tag{6}$$

$$\begin{aligned}\mathbf{P}_{\mathrm{x}_k}^- &= \frac{1}{4\ell^2}\sum_{i=1}^{L_x}[f(\hat{\mathbf{x}}_{k-1} + \mathbf{s}_{k-1}^{x,i}, \overline{\mathbf{w}}_k, \mathbf{u}_{k-1}) - f(\hat{\mathbf{x}}_{k-1} - \mathbf{s}_{k-1}^{x,i}, \overline{\mathbf{w}}_k, \mathbf{u}_{k-1})]^2 \\ &+ \frac{1}{4\ell^2}\sum_{i=1}^{L_w}[f(\hat{\mathbf{x}}_{k-1}, \overline{\mathbf{w}}_k + \mathbf{s}_{k-1}^{w,i}, \mathbf{u}_{k-1}) - f(\hat{\mathbf{x}}_{k-1}, \overline{\mathbf{w}}_k - \mathbf{s}_{k-1}^{w,i}, \mathbf{u}_{k-1})]^2 \\ &+ \frac{\ell^2 - 1}{4\ell^2}\sum_{i=1}^{L_x}[f(\hat{\mathbf{x}}_{k-1} + \mathbf{s}_{k-1}^{x,i}, \overline{\mathbf{w}}_k, \mathbf{u}_{k-1}) + f(\hat{\mathbf{x}}_{k-1} - \mathbf{s}_{k-1}^{x,i}, \overline{\mathbf{w}}_k, \mathbf{u}_{k-1}) \\ &- 2f(\hat{\mathbf{x}}_{k-1}, \overline{\mathbf{w}}_k, \mathbf{u}_{k-1})]^2 \\ &+ \frac{\ell^2 - 1}{4\ell^2}\sum_{i=1}^{L_w}[f(\hat{\mathbf{x}}_{k-1}, \overline{\mathbf{w}}_k + \mathbf{s}_{k-1}^{w,i}, \mathbf{u}_{k-1}) + f(\hat{\mathbf{x}}_{k-1}, \overline{\mathbf{w}}_k - \mathbf{s}_{k-1}^{w,i}, \mathbf{u}_{k-1}) \\ &- 2f(\hat{\mathbf{x}}_{k-1}, \overline{\mathbf{w}}_k, \mathbf{u}_{k-1})]^2\end{aligned} \tag{7}$$

Now, before calculating the measurement update, covariance square-root column vectors for measurement-update must be calculated.

$$\mathbf{s}_{k-1}^{x,i} = \ell\left(\sqrt{\mathbf{P}_{\mathrm{x}_k}^-}\right)_i \qquad i = 1, 2, \ldots, L \tag{8}$$

$$\mathbf{s}_{k-1}^{v,i} = \ell\left(\sqrt{\mathbf{R}_k}\right)_i \qquad i = 1, 2, \ldots, L_{\mathrm{v}} \tag{9}$$

Measurement update equations are calculated as follows

$$\begin{aligned}\hat{\mathbf{z}}_k^- &= \frac{\ell^2 - L_x - L_{\mathrm{v}}}{\ell^2} h(\hat{\mathbf{x}}_k, \overline{\mathbf{v}}_k) \\ &+ \frac{1}{2\ell^2}\sum_{i=1}^{L_x}[h(\hat{\mathbf{x}}_k^- + \mathbf{s}_k^{x,i}, \overline{\mathbf{v}}_k) + h(\hat{\mathbf{x}}_k^- - \mathbf{s}_k^{x,i}, \overline{\mathbf{v}}_k)] \\ &+ \frac{1}{2\ell^2}\sum_{i=1}^{L_v}[h(\hat{\mathbf{x}}_k^-, \overline{\mathbf{v}}_k + \mathbf{s}_k^{v,i}) + h(\hat{\mathbf{x}}_k^-, \overline{\mathbf{v}}_k - \mathbf{s}_k^{v,i})]\end{aligned} \tag{10}$$

$$\begin{aligned}\mathbf{P}_{\hat{\mathrm{y}}_k}^- &= \frac{1}{4\ell^2}\sum_{i=1}^{L_x}[h(\hat{\mathbf{x}}_k^- + \mathbf{s}_k^{x,i}, \overline{\mathbf{v}}_k) - h(\hat{\mathbf{x}}_k^- + \mathbf{s}_k^{x,i}, \overline{\mathbf{v}}_k)]^2 \\ &+ \frac{1}{4\ell^2}\sum_{i=1}^{L_v}[h(\hat{\mathbf{x}}_k^-, \overline{\mathbf{v}}_k + \mathbf{s}_k^{v,i}) - h(\hat{\mathbf{x}}_k^-, \overline{\mathbf{v}}_k - \mathbf{s}_k^{v,i})]^2 \\ &+ \frac{\ell^2 - 1}{4\ell^2}\sum_{i=1}^{L_x}[h(\hat{\mathbf{x}}_k^- + \mathbf{s}_k^{x,i}, \overline{\mathbf{v}}_k) + h(\hat{\mathbf{x}}_k^- - \mathbf{s}_k^{x,i}, \overline{\mathbf{v}}_k) - 2h(\hat{\mathbf{x}}_k^-, \overline{\mathbf{v}}_k)]^2 \\ &+ \frac{\ell^2 - 1}{4\ell^2}\sum_{i=1}^{L_v}[h(\hat{\mathbf{x}}_k^-, \overline{\mathbf{v}}_k + \mathbf{s}_k^{x,i}) + h(\hat{\mathbf{x}}_k^-, \overline{\mathbf{v}}_k - \mathbf{s}_k^{x,i}) - 2h(\hat{\mathbf{x}}_k^-, \overline{\mathbf{v}}_k)]^2\end{aligned} \tag{11}$$

$$\mathbf{P}_{\mathrm{x}_k\mathrm{y}_k} = \frac{1}{4\ell^2}\sum_{i=1}^{L_x}\mathbf{s}_k^{x,i}[h(\hat{\mathbf{x}}_k^- + \mathbf{s}_k^{x,i}, \overline{\mathbf{v}}_k) - h(\hat{\mathbf{x}}_k^- - \mathbf{s}_k^{x,i}, \overline{\mathbf{v}}_k)]^T \tag{12}$$

$$\mathbf{K}_k = \mathbf{P}_{\mathrm{x}_k\mathrm{y}_k}\mathbf{P}_{\hat{\mathrm{y}}_k}^{-1} \tag{13}$$

$$\hat{\mathbf{x}}_k = \hat{\mathbf{x}}_k^- + \mathbf{K}_k(\mathbf{y}_k - \hat{\mathbf{y}}_k^-) \tag{14}$$

$$\mathbf{P}_{\mathrm{x}_k} = \mathbf{P}_{\mathrm{x}_k}^- - \mathbf{K}_k\mathbf{P}_{\hat{\mathrm{y}}_k}\mathbf{K}_k^T \tag{15}$$

Parameters are the scalar central difference interval size. For Gaussian x, the optimal value is Lx, Lw, and Lv are the dimensions of the state, process noise and observation noise respectively. Q_k is the covariance matrix of motion noise and R_k is the covariance matrix of the observation noise. $(.)^2$ is the

shorthand for the vector outer product, i.e. a^2 = a.a, and is the ith column of the matrix square root of the square-symmetric matrix P (Norgard et al, 2000).

4 SIMULATIONS AND RESULTS

A. Evolution of the map

The range bearing sensor mounted on the robot returns the distance between the sensor and the landmark as well as the angle between the robot's frame of reference and the landmark's frame of reference. Since all landmarks are considered static in the environment, the reference frame of landmarks is the same as global frame of reference. The measurement information related to a landmark is in form of polar measurement (D, β), indicating range and bearing angle of the landmark. In the global frame of reference, the landmark coordinate is referred by (x, y). In a standard filter (such as EKF) the first order Taylor series truncation is used to linearize this nonlinear observation model by which the calculation of any possible error becomes significantly inaccurate.

B. Robustness

As depicted in figure 1, the landmark position located at (x=50.2 , y=149.8) is estimated by incorporating range and bearing data (*D, β*) received by the range/bearing sensor. In this case, zero-mean Gaussian noise is added and the data is converted to the Cartesian plane. As a result of low accuracy in estimation of the bearing direction, samples appear in form of banana shapes. As shown in figures 1-a, 1-b, and 1-c, the estimated mean and covariance of this distribution is relatively far from the true mean and covariance of the system. The estimation of the mean and covariance in the UHS algorithm is shown in figure 1-d which appears as the most accurate estimation among all filters. The inaccuracy in estimation of the mean in the range and the covariance in FastSLAM algorithm, usually results in the over estimation of the posterior distribution in the range which leads the filter to become over confident. HybridSLAM would produce an inaccurate mean and covariance since the linearization is based on the first order of Taylor series (Julier, Uhlmann, 2001). As long as the map has a small size, all filters tend to approximate the mean and covariance of the system reasonably.

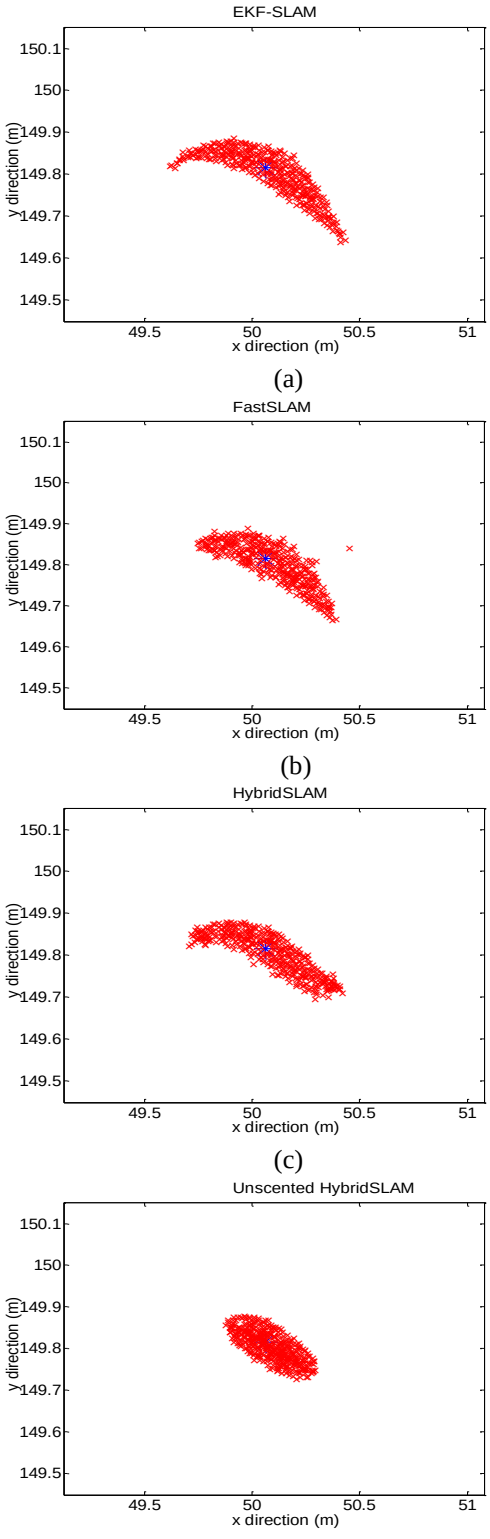

Figure 1: Estimation of the mean and covariance of a landmark a) EKF-SLAM b) FastSLAM c) HybridSLAM d) Unscented HybridSLAM

Once the track becomes large, EKF fails to estimate an accurate map and both FastSLAM and HS become overconfident. Unlike the other three filters, UHS performs with minimum error in the mean and the covariance estimate which indicates high accuracy and the robustness of the filter.

C. Map fusion

In order to demonstrate how the map is evolved in the estimation process, a scenario is simulated in this section. Figure 2 illustrates an environment with a few landmarks gathered in small groups. The vehicle velocity is set on 2 m/s and the range for the range/bearing laser is 10 meters. As the vehicle starts localizing from point (0, 0), two landmarks at locations (x=2.3,y=5.2) and (x=5.0,y=3.6) are observed by the range finder. These landmarks are the first features observed in the vicinity of the vehicle, building the first piece of the map using subordinate filter FastSLAM. At the same time, UKF is building the same map independently. Once the first piece of the map is estimated by both filters, the map built by FastSLAM will be added to the global map and at the same time, the uncertainty difference between sub-filter estimations will be taken into account. Once the robot observes first set of landmarks in the vicinity, the first region is added to the global map. The Constraint Local Sub-map Filter (CLSF) constraint [7] would compare the map estimated by the particle filter to a map produced by UKF. This is the very important stage to choose one map estimated over the other one. Depending on how accurate the map is constructed, a final decision is made and the first local map is added to the global map. In figure 3 the region added to the map is shown by a rectangle and the new region is under observation. Robot is approximately at the coordinate (10, 0). The first region inside the square is already a part of the global map. The robot is observing the second region consisting of only one landmark. Same as the first region, the map of the new region is built by both subordinate filters and through CLSF the decision is made to add the most updated and accurate map to the global map.

Once the second region in the vicinity of the robot is estimated, it is also evaluated by CLSF which has already included the map by UKF. The decision is now based on the CLSF algorithm evaluation to compare the two maps built by different filters. If the map built by UKF is not crossing its threshold, it remains as is. If CLSF figures out that the map built by FastSLAM is more accurate relative to the one built by UKF, the accurate map is used. Figure 4 demonstrates the new area surrounded by a plaque and added to the global map. The first and second regions of the map are identified and part of the global map. The robot starts observing the third region from point (23, 3) with respect to the global map. The first and second regions are now correlated and have a critical role for the next decision making by CLSF. It should be noted that at this point, the first region is correlated with the second region and as a whole map, regions are expecting for the third region to be added to the map in order to complete the map up to that time step. In Unscented HybridSLAM algorithm, the local mapping is occurring and at the same time the map built by UKF is supporting the whole mapping process ((Julier, Uhlmann, 2004).

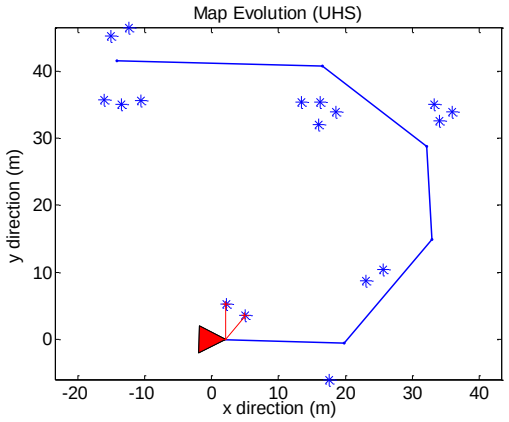

Figure 2: Robot at coordinate (0,0)

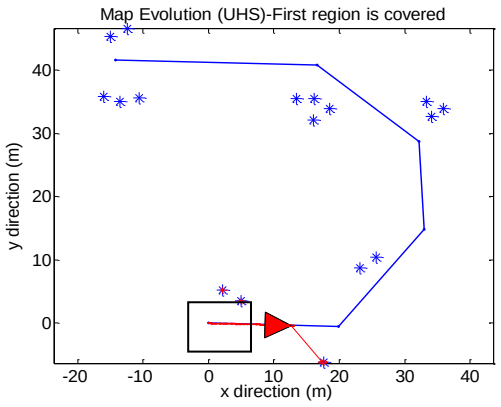

Figure 3: Robot is approximately at the coordinate (10, 0)

Usually in the EKF-SLAM sub-algorithm of HS, spurious observations are associated with landmarks, particularly during transient periods of high vehicle uncertainty. It should be noted that the Failures as the result of the EKF filter in HS does not happen in the proposed algorithm in similar scenarios. Even though the landmark is not observed simultaneously, the ambiguity can be resolved. The local linearization error is another failure mode of EKF-SLAM which is not occurring when it is replaced by UKF. When the UKF algorithm begins to build a local map, the linearization error is at its minimum level. As a result, the uncertainty becomes small. In such case where the local-map uncertainty can be significant, the robustness of the UHS would cover any possible fault by integrating spurious observations of data association information of the observed landmark over time (Bailey et al, 2006). In figure 5 the correlation of three identified regions of the map is shown. The robot is approximately at point (33, 26) and observing the fourth region in the vicinity. Same process will follow to add a new piece to the map. The third region is indicated by a trapezoid and contains two individual landmarks.

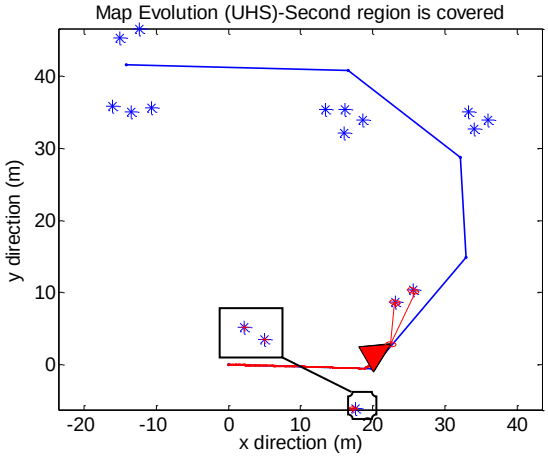

Figure 4: Robot starts observing the third region from point (23, 3) with respect to the global map.

t

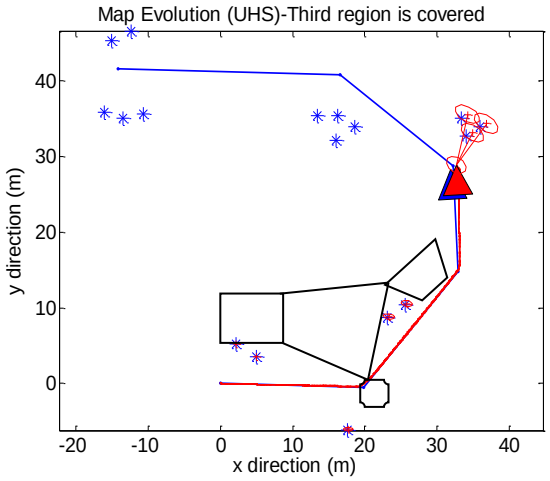

Figure 5: Robot is approximately at point (33, 26) and observing the fourth region in the vicinity.

D. Map Update

Figure 6 demonstrates a loop closing scenario in a domestic environment utilizing edges as line segments. The environment is a 50m by 50m area and the starting point is set on the global coordination (x=11,y=29). Edges are composed of approximately 1.00m distant landmarks by which lines at the corners of the environment are represented. In this simulation, map update process is demonstrated through sequential figures. The sensor installed on the robot returns the range and bearing information to landmarks in the environment. The sensor range for this simulation is set to 20 meters and vehicle speed is set to 2 m/s. As shown in figure 6, the robot arrives at waypoint 2, estimating and updating the map of the environment. Black dots around landmarks indicate estimated locations of landmarks that are not incorporated into the map fusion process. At some point, the location of a particular landmark is over-estimated either by the FastSLAM sub-filter or by the UKF sub-filter. In this case, CLSF decides not to fuse that information into the global map and instead, updates the map with the previous data. On the other hand, if the estimation is not beyond some threshold, location of a landmark is fused to the global map, and as a result, becomes part of the absolute map that the system can rely on for the next time steps.

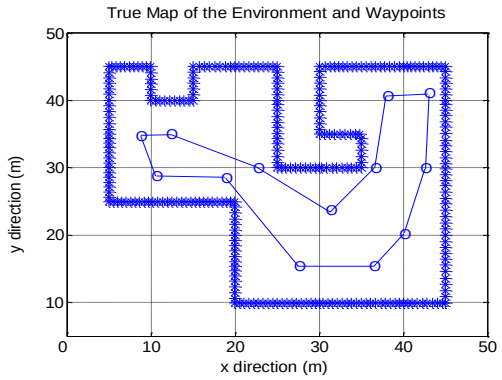

Figure 5: True map of a 50m by 50m environment in which waypoints are set. Waypoints are connected by straight lines showing an imaginary path.

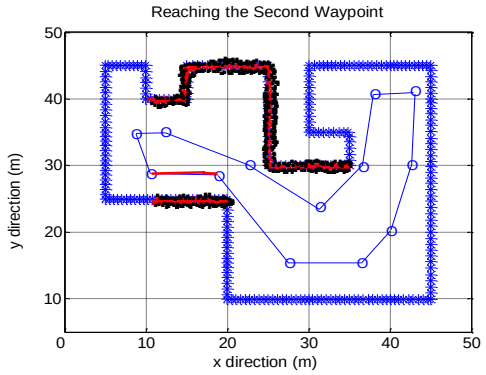

Figure 6: Robot is at the second waypoint

In figure 7, the robot is arrived at the sixth waypoint. More landmarks at the range of the sensor are observed and the map is still built using both suboptimal filters and with a final supervision of CLSF. As the process goes on, landmarks that have been observed in previous time steps are re-observed from the new robot locations, and help the system to ignore previous wrong estimations. Black "dots" and red "crosses" in this picture are changing their locations as the process proceeds. Figures 8 and 9 illustrate the resulting map at the tenth waypoint and at the end of the loop closing. Figure 10 demonstrates the final version of the map built during the loop closing indicating that the map update process has been successful using UHS. This map is now considered as the basis for global map referenced for the next cycle. Figures 11 and 12 show the RMS position and orientation error regarding the scenario depicted in figure 9. For this simulation, 300 particles are used and the vehicle velocity is set to 1.5m/s. RMS position error remains around 0.35m in average and the orientation error, in average is around 0.02 radians. The UHS algorithm appears to perform with a high accuracy in this case.

Once the loop is closed, the map produced at the end of the loop will be used as a referenced map (global) for the next loop. It is very important to mention that at the beginning of the second loop, the SLAM problem may be treated as just a localization problem.

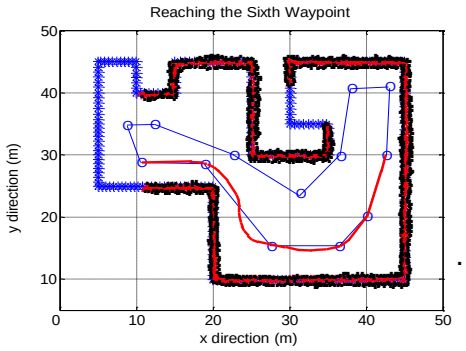

Figure 7: Sixth waypoint is reached by the robot and the map is built by suboptimal filters and the CLSF.

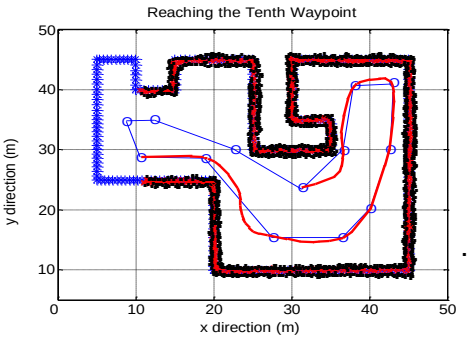

Figure 8: Robot is at the tenth waypoint

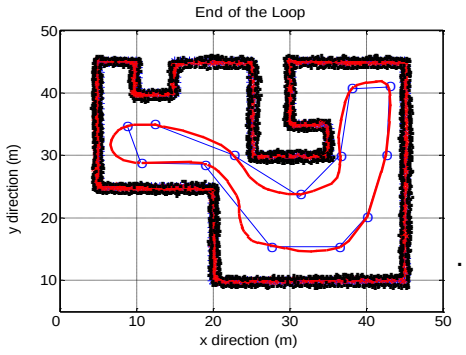

Figure 9: End of the first loop

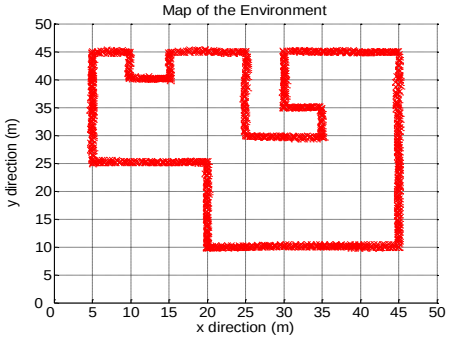

Figure 10: Map of the environment is built prior to the next loop

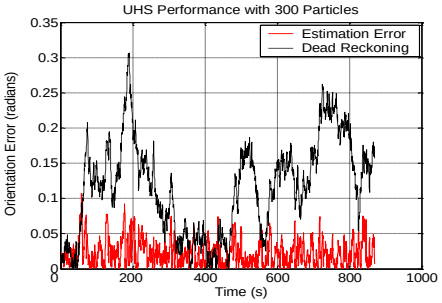

Figure 11: Orientation error is 0.02 radians in average for the SLAM process using UHS

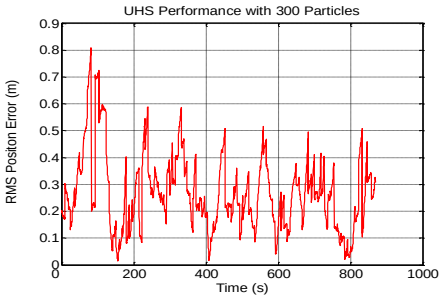

Figure 12: RMS position error is 0.35m in average for the SLAM process using UHS

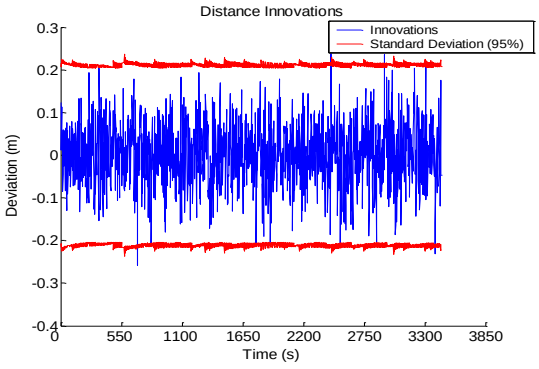

Figure 13: Standard deviation vs. distance innovation

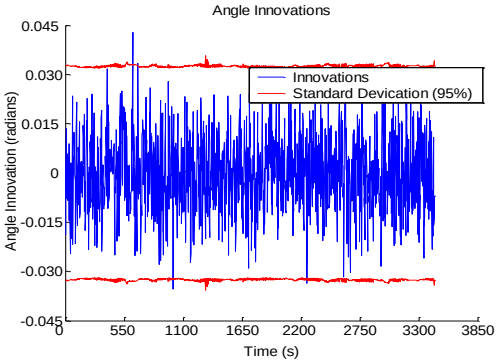

Figure 14: Standard deviation vs. angle innovation

Figures 13 and 14 depict the 2-sigma standard deviation (95%) vs. the innovation in terms of vehicle heading angle as well as its distance. Simulations show that the mean remains close to zero which results in a reliable and consistent map even though the loop is completed. Results show, as long as the ambiguity of data association is reduced by the UHS, a compact map configuration does not affect the performance of the filter, and the results would be identical to a SLAM case with a regular loop closing case. This is important since filters such as EKF fail to fulfill the navigation task in such circumstances.

CONCLUSION

The main contribution of this study is a thorough investigation and the validity check of Unscented HybridSLAM. Simulations of the vehicle trajectory and the estimation accuracy are investigated based on proposed algorithm. The map accuracy and path estimation are compared to currently used algorithms, in particular, resulting in high quality of the produced map and reducing error in estimated position and robot heading. Results from different scenarios indicate that the proposed algorithm is be able to handle hundreds of nearby landmarks with minimum data association ambiguity and a high level of accuracy in the path estimation when compared to currently used algorithms.

ACKNOWLEDGEMENT

An academic version of a free software for robotics research was used in this study. The software in

form of both MATLAB and C++ codes is available at http://www.lasmea.univ-bpclermont.fr/ftp/pub/trassou/SLAM/SLAM_Summer_School2002/SLAM%20Summer%20School%202002.htm

REFERENCES

Smith R., Cheeseman P., 1986, The estimation and representation of spatial uncertainty, International Journal of Robotics Research, Vol. 5, Issue 4, pp. 56-68.

Durrant-Whyte H., Bailey T., 2006, Simultaneous localization and mapping (SLAM): part I the essential algorithms, IEEE Robatics and Automation Magazine, Vol. 13, No. 2, pp. 99-108, June.

Monjazeb A., Sasiadek J. Z., Necsulescu D., 2012, An approach to autonomous navigation based on Unscented HybridSLAM, Proc. of 17th International Conference on Methods and Models in Automation and Robotics, pp. 369-374, Miedzyzdroje, Poland.

Montemerlo M., Thrun S., 2003, Simultaneous localization and mapping with unknown data association using FastSLAM, Proceedings of the IEEE International Conference on Robotics and Automation, pp. 1985-1991, Vol. 2, September.

Bailey T., Mobile robot localization and mapping in extensive outdoor environments, 2002, PhD Thesis, Australian Centre for Field Robotics, University of Sydney, Sydney, Australia.

Brooks A., Bailey T., 2009, HybridSLAM: Combining FastSLAM and EKF-SLAM for reliable mapping, Springer Tracts in Advanced Robotics, Volume 57, pp. 647-661.

Williams S. B., Dissanayake G., Durrant-Whyte H., 2002, An Efficient Approach to the Simultaneous Localisation and Mapping Problem, Proceedings of the IEEE International Conference on Robotics & Automation, Washington DC.

Monjazeb A., Sasiadek J. Z., Necsulescu D., 2014, Navigation of an Autonomous Mobile Robot Using Data Association Method, Proc. of 11th International Conference on Informatics in Control, Automation and Robotics (ICINCO), pp. 304 - 311, Vienna, Austria.

Monjazeb A., Sasiadek J. Z., Necsulescu D., 2011, Autonomous navigation among large number of nearby landmarks using FastSLAM and EKF-SLAM; a comparative study, Proc. of 16th International Conference on Methods and Models in Automation and Robotics (MMAR), pp. 369-374, Miedzyzdroje, Poland.

Norgard M., Poulsen N., Ravn O., 2000, New development in state estimation for nonlinear systems, IFAC Automatica, pp. 1627-1638, Vol. 36, No. 11, November.

Julier S. J., Uhlmann J. K., 2001, A counter example to the theory of simultaneous localization and map building, Proc. of IEEE International Conference on Robotics and Automation, pp. 4238-4243, March.

Julier S. J., Uhlmann J. K., 2004, Unscented filtering and nonlinear estimation, Proc. of IEEE Journal, Vol. 92, Issue 3, pp. 401-422, March.

Bailey T., Nieto J., Nebot E., 2006, Consistency of FastSLAM algorithm, Proceedings of IEEE International Conference on Digital Object Identifier, pp. 424-429.